Journal Pre-proof

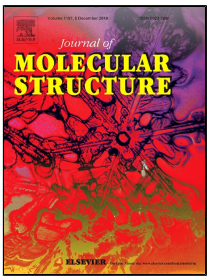

Synthesis, crystal structure, and non-covalent interactions in 4-hydrazinobenzoic acid hydrochloride.

Miguel Morales-Toyo, Néstor Cubillán, Christopher Glidewell, Luis Seijas, Katerin Boscan-Melean, Jelen Restrepo

PII:	S0022-2860(19)31263-3
DOI:	https://doi.org/10.1016/j.molstruc.2019.127154
Reference:	MOLSTR 127154
To appear in:	*Journal of Molecular Structure*
Received Date:	31 May 2019
Accepted Date:	27 September 2019

Please cite this article as: Miguel Morales-Toyo, Néstor Cubillán, Christopher Glidewell, Luis Seijas, Katerin Boscan-Melean, Jelen Restrepo, Synthesis, crystal structure, and non-covalent interactions in 4-hydrazinobenzoic acid hydrochloride., *Journal of Molecular Structure* (2019), https://doi.org/10.1016/j.molstruc.2019.127154

Synthesis, crystal structure, and non-covalent interactions in 4-hydrazinobenzoic acid hydrochloride.

Miguel Morales-Toyo,[1,2*] Néstor Cubillán,[3] Christopher Glidewell,[4] Luis Seijas,[5] Katerin Boscan-Melean,[6] Jelen Restrepo.[6**]

[1]Laboratorio de Electrónica Molecular (LEM), Departamento de Química, Facultad Experimental de Ciencias, La Universidad del Zulia, Ap. 526, Grano de Oro, Módulo No. 2, Maracaibo, Estado Zulia, Bolivarian Republic of Venezuela.

[2]Facultad de Humanidades, Universidad Adventista Dominicana (UNAD), Autopista Duarte Km 74 ½, Villa Sonador, Provincial Monseñor Nouel, 42000, República Dominicana.

[3]Programa de Química, Universidad del Atlántico, Barranquilla, Colombia.

[4]School of Chemistry, University of St Andrews, St Andrews, Fife KY16 9ST, UK.

[5]Laboratorio de Procesos Dinámicos en Química, Departamento de Química, Facultad de Ciencias, Universidad de Los Andes, 5101 Mérida, República Bolivariana de Venezuela.

[6]Laboratory of Molecular and Biomolecular Characterization, Center for Research in Materials Technology (CITeMA), Venezuelan Institute of Scientific Research (IVIC), Bolivarian Republic of Venezuela.

Email: *miguelmorales@unad.edu.do; **jrestrepo@ivic.gob.ve

ABSTRACT

The compound 4-hydrazinobenzoic acid hydrochloride (4-HBA), $C_7H_9O_2.Cl$, has been synthesized and characterized by FT-IR spectroscopy and X-ray diffraction. The compound crystallizes as colourless needles in a triclinic system, space group $P\bar{1}$ (Z=2), and cell parameters a = 3.7176 (4) Å, b = 5.9133 (4) Å, c = 19.3631 (13) Å, α = 87.841 (6), β = 88.924 (6), γ = 80.203 (6), V = 419.13 (6) Å^3. The component ions are linked by a combination of O-H...O, N-H...N and N-H...Cl hydrogen bonds to form a complex three-

dimensional framework structure in which each cation is linked to two other cations, by O-H...O and N-H...N hydrogen bonds, and to five different anions, while each anion accepts hydrogen bonds from five different cations. Calculations on the Non-Covalent Interactions (NCI) amplify the crystallographic conclusions concerning the interionic hydrogen bonds.

Keywords: Phenylhydrazine hydrochloride, synthesis, crystal structure, non-covalent interactions.

1. Introduction

Phenylhydrazine (PHZ) was the first hydrazine derivative characterized by H. E. Fisher in 1875.[1] At the end of the 19th century, its early field of application was mainly a pharmaceutical drug, e.g. PHZ has been used to clinically treat *polycythemia vera*, and as antipyretic. However, it is no longer used both because of the appearance of more effective therapies and because of its toxicity.[2]

4-Hydrazino benzoic acid (4-HBA) is a derivative of PHZ, it is a known genotoxin and carcinogen in rat and mice.4-HBA is often used in drug manufacturing as a counter-ion, acid catalyst or an easy-removal protecting group in the course of the synthesis. The potential presence of these genotoxins in manufactured drugs has attracted attention of regulatory authorities.[3]

In addition, compounds of this type are used worldwide as chemical intermediate in the synthesis of several heterocycles, hydrazones, hydrazides, thiosemicarbazone and semicarbazone compounds.[4–9] For example, In the Fischer indole synthesis, functionalized indoles are obtained from PHZ and cyclohexanone under mild conditions in a tartaric acid-dimethylurea melt (Scheme 1).[10,11]

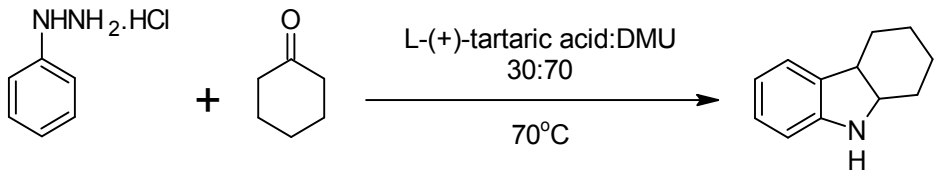

Scheme 1. Synthesis of functionalized indoles.[12]

On the other hand, PHZ derivatives under acidic conditions react with ketones or aldehydes to form hydrazone derivatives (Scheme 2).[13] In previous works, we have synthesized 4-HBA and ethyl 4-hydrazinobenzoate hydrochloride (E-4HB) as intermediates to produce furan-2- and thiophen-2-phenylhydrazones from its aldehydes, in order to study their interactions with biomolecules such as DNA and HSA by using spectroscopic and molecular docking techniques.[6,14,15]

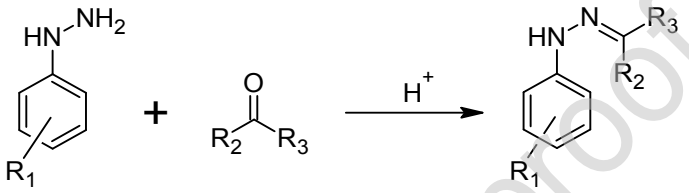

Scheme 2. Synthesis of hydrazone derivatives.[6,12,13]

Nowadays, crystallography provides the strongest experimental evidence for interactions between atoms and molecules. However, sometimes it becomes necessary to use complementary information in order to gain insights about underlying interactions.

Recently, quantum chemistry methods have been increasingly used for the in depth exploration of these interactions.[16], allowing the quantitative partition of the interaction energy (E_{int}) into five contributions, namely electrostatic (ΔE_{el}), exchange (ΔE_{ex}), repulsion (ΔE_{rep}), polarization (ΔE_{pol}) and dispersion (ΔE_{dis}). Using this approach, called Localized Molecular Orbital Energy Decomposition Analysis (LMO-EDA), a detailed study of the physical origin of the noncovalent interactions is performed.[17]

On the other hand, the study of non-covalent interactions through the reduced gradient of density (NCIPlot) has gained popularity because of the advantages of this method in the characterization and location of interactions in molecular real-space.[18,19] The combination of these methods with those of X-ray crystallography have been important in identifying the basis of supramolecular structures, e.g. Hernandez-Paredes found the role of

C-H•••O interaction in the assembly of 5-methoxy-2-nitroaniline and its co-crystal with 2-amino-5-nitropyridine.[20] Consequently, this approach has gained popularity as a complement to crystallographic studies.

Based on these considerations, we report here the synthesis and crystal structure of 4-HBA hydrochloride studied by X-ray diffraction technique. Additionally, a discussion of the NCI in terms of LMO-EDA and NCIPlot was presented.

2. Experimental

2.1. General procedure and materials

Melting points were determined on a digital IA-9100 ELECTROTHERMAL Fusiometer. The IR spectrums were recorded on a Shimadzu Model IR Prestige21 FT-IR Spectrometer in a KBr pellets. X-ray diffraction data were collected using a *KAPPA DUO PAEXII* diffractometer.

2.2. Synthesis of 4-Hydrazinobenzoic acid hydrochloride (4-HBA).

The synthesis of the tittle compound comprises two steps: (2.2.1) Preparation of diazonium salt from *p*-aminobenzoic acid (PABA) and (2.2.2) reduction of diazonium salt with H_2SO_3(aq) (Scheme 3). [14,21,22]

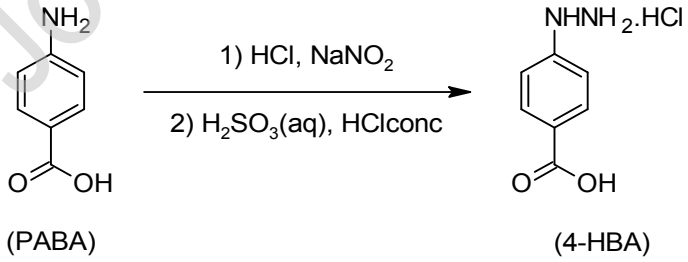

Scheme 3. Synthesis of 4-HBA.[12,14]

2.2.1. Preparation of diazonium salts

A 100 mL round-bottom flask with magnetic stirring was charged with 7.5 mmol (1.03 g) of PABA suspended in 7 mL of distilled H_2O and cooled with an ice-salt bath. Then, 8.1 mL of concentrated HCl were added and the mixture let to cool to 0 ºC. After, a solution of sodium nitrite (7.5 mmol, 0.518 g in 5 mL of distilled H_2O) was slowly added (~30 min) using a dropping funnel and the stirring process continued by 15 min longer. The clear orange resulting solution (diazonium salt) was diluted with 15 mL of distilled H_2O.[21,23]

2.2.2. Reduction of diazonium salts with H_2SO_3(aq)

In a 500 mL round-bottom flask, surrounded by an ice-salt bath, a solution of H_2SO_3 was prepared by saturating SO_2 gas in 60 mL of distilled H_2O at 0-5 °C. Under the gas stream, the cold diazonium salt solution was added in aliquots of 3 mL every 15 minutes keeping the temperature between 5 and 10 °C. After the reaction mixture becomes dark, the SO_2 stream was keep by 20 min longer without the cooling bath. The mixture was chilled to 0-5 °C by 12 hours after addition of 71 mL of concentrated HCl. The product 4-HBA was collected by filtration, and washed with two portions of 10 mL of cold concentrated HCl.[21]

The title compound was recrystallized from 10 mL distilled H_2O and 1 mL concentrated HCl and let boil for a short time with activated charcoal. After filtering, 1 mL of concentrated HCl were added; the mixture cooled to 0 °C, and finally the 4-HBA were collected by filtration.[21] This product was obtained as white needles and it was suitable for the diffraction analysis without further treatment.

2.3. Crystal structure determination

Crystal data, data collection and structure refinement details are summarized in Table 1: standard software was used throughout.[24–28] All H atoms were located in difference maps. The H atoms bonded to C atoms were then treated as riding atoms in geometrically idealized positions with C-H distances 0.95 Å and with $U_{iso}(H) = 1.2U_{eq}(C)$. For the H atoms bonded to N or O atoms, the atomic coordinates were refined, with $U_{iso}(H) = 1.2U_{eq}(N)$ or $1.5U_{eq}(O)$, giving the N-H and O-H distances shown in Table 2.

Table 1. Experimental details.

4-HBA	
Crystal data	
Chemical formula	$C_7H_9N_2O_2 \cdot Cl$
M_r	188.61
Crystal system, space group	Triclinic, $P\bar{1}$
Temperature (K)	100
a, b, c (Å)	3.7176 (4), 5.9133 (4), 19.3631 (13)
α, β, λ (°)	87.841 (6), 88.924 (6), 80.203 (6)
V (Å^3)	419.13 (6)
Z	2
Radiation type	Mo $K\alpha$
μ (mm^{-1})	0.41
Crystal size (mm)	0.10 × 0.08 × 0.08
Data collection	
Diffractometer	Bruker D8 Venture
Absorption correction	Multi-scan *SADABS2012*/1 (Bruker, 2012)
T_{min}, T_{max}	0.885, 0.967
No. of measured, independent and observed [$I > 2\sigma(I)$] reflections	5191, 1477, 1366
R_{int}	0.039
$(\sin \theta/\lambda)_{max}$ (Å^{-1})	0.596
Refinement	
$R[F^2 > 2\sigma(F^2)]$, $wR(F^2)$, S	0.034, 0.110, 1.13
No. of reflections	1477
No. of parameters	124
H-atom treatment	H atoms treated by a mixture of independent and constrained refinement
$\Delta\rangle_{max}$, $\Delta\rangle_{min}$ (e Å^{-3})	0.35, -0.38

Table 2. Parameters (Å, º) for hydrogen bonds.

D-H...A	D-H	H...A	D...A	D-H...A	Symmetry
O1-H1...O2	0.93(3)	1.69(3)	2.622(2)	178(4)	-x,1-y,-z
N41-H41...Cl1	0.79(3)	2.68(3)	3.3048(19)	138(2)	-x,-y,1-z
N41-H41...Cl1	0.79(3)	2.70(3)	3.2919(19)	134(2)	1-x,-y,1-z
N42-H42A...Cl1	0.98(3)	2.19(3)	3.1082(18)	156(2)	x,y,z
N42-H42B...N41	0.84(3)	2.17(3)	3.002(3)	173(2)	1+x,y,z
N42-H42C...Cl1	0.89(3)	2.43(3)	3.1862(19)	143(2)	-x,1-y,1-z
N42-H42C...Cl1	0.89(3)	2.70(3)	3.2650(19)	122(2)	1-x,1-y,1-z

3. Computational details

The noncovalent interactions observed by X-ray crystallography were assessed by analyzing the topology of density, ρ(r) [Quantum Theory of Atoms in Molecule, QTAIM], and the reduced gradient of ρ(r) [NCIPlot] and LMO-EDA calculations. The unit cell and two structural models without further geometry optimization were used to represent the most important intermolecular interactions in the crystal, i.e., electrostatics, hydrogen bond and π-stacking. QTAIM calculation were performed with Multiwfn 3.6.[29] The reduced gradient of ρ(r) calculations were carried-out using NCIplot 3.0 with the promolecular approach and the densities obtained by DFT.[18,19] Calculations ion unit cell were performed with Critic2.[30] NCIRange allowed us to extract the important region of interaction.[31] All isosurfaces were graphed with VMD.[32]

The LMO-EDA calculations on the crystallographic structures of the unit cell and molecular motifs were performed with GAMESS.[33] In GAMESS, LMO-EDA was recently adapted to work with canonical orbitals, and named canonical molecular orbital energy decomposition analysis (CMO-EDA). The DFT calculations were carried-out with the M06-2X/aug-cc-pVDZ level of theory. The use of this functional is supported by the results of the interaction energy of molecules from Benchmark Energy and Geometry Database with several functional reported by Li et al.,[34] and Brauer et al.[35] In relation to the basis sets, Hobza founds the lesser error with aug-cc-pVTZ basis set for 66 molecular complexes by using CCSD(T) method.[36] However, the author showed differences around

0.1 kcal/mol when aug-cc-pVDZ was used. On these bases, and attending the compromise of accuracy and computing time, we calculated the electronic structure with the level of theory mentioned at the top of this paragraph.

4. Results and discussion

4.1. Synthesis and spectroscopy characterization of 4-HBA.

The title compound 4-HBA was synthetized from PABA (Scheme 3) according to the procedures 2.2.1 and 2.2.2. Yield = 91%, white needles, mp = 245 °C (dec). FTIR (KBr, disk) cm^{-1}: 3211.3 (N-H), 2500-3300 (-CO_2H), 1685.7 (C=O), 1612.4 (C=C), 1240.1 (C-O-C).

4.2. Structure description.

The compound 4-HBA is a salt in which the hydrazine is protonated at the terminal N atom, and in the selected asymmetric unit (Figure 1), the two ionic components are linked by an N-H...Cl hydrogen bond (Table 2). Overall, the ions are linked into a complex three-dimensional framework structure by an extensive series of hydrogen bonds. Inversion-related pairs of cations are linked by paired O-H...O hydrogen bonds to form an $R^2_2(8)$ motif, so forming a centrosymmetric four-ion aggregate which can be regarded as the basic building block for the overall supramolecular assembly.[37] These aggregates are then further linked by a nearly-linear two-centre N-H...N hydrogen bond, involving atom H42B, and two independent planar three-centre N-H...$(Cl)_2$ hydrogen bonds; that involving atom H41 is nearly symmetrical, but that involving H42C is markedly asymmetric (Table 2); based upon these interactions, the formation of the three-dimensional assembly can readily be analyzed in terms of simple, one-dimensional sub-structures: the choice of these is to some extent arbitrary, but we select here the simplest group of such sub-structures.

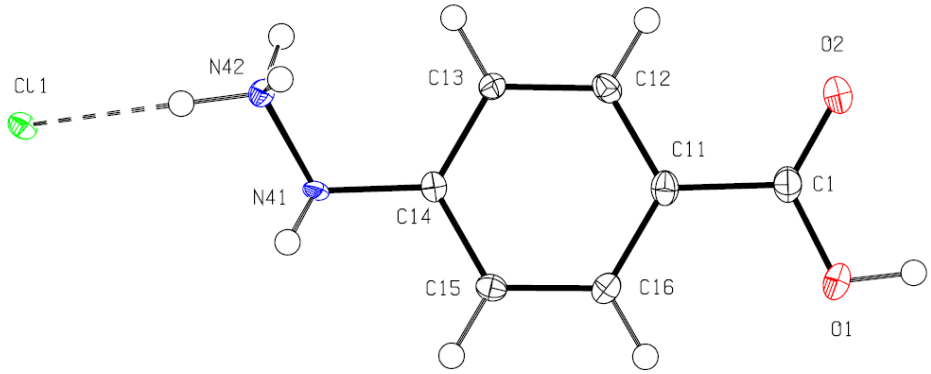

Figure 1. The molecular structure of the compound 4-HBA showing the atom-labelling scheme and the N-H..Cl hydrogen bond linking the two ions within the selected asymmetric unit. Displacement ellipsoids are drawn at the 50% probability level.

The N-H...N hydrogen bond links four-ion aggregates which are related by translation to form a ribbon, or molecular ladder, running parallel to the [100] direction. The rungs of the ladder comprise two antiparallel C(3) chains, while rungs of the ladder consists of cation dimer units containing $R^2_2(8)$ rings, with $R^4_4(34)$ rings between the rungs (Figure 2).

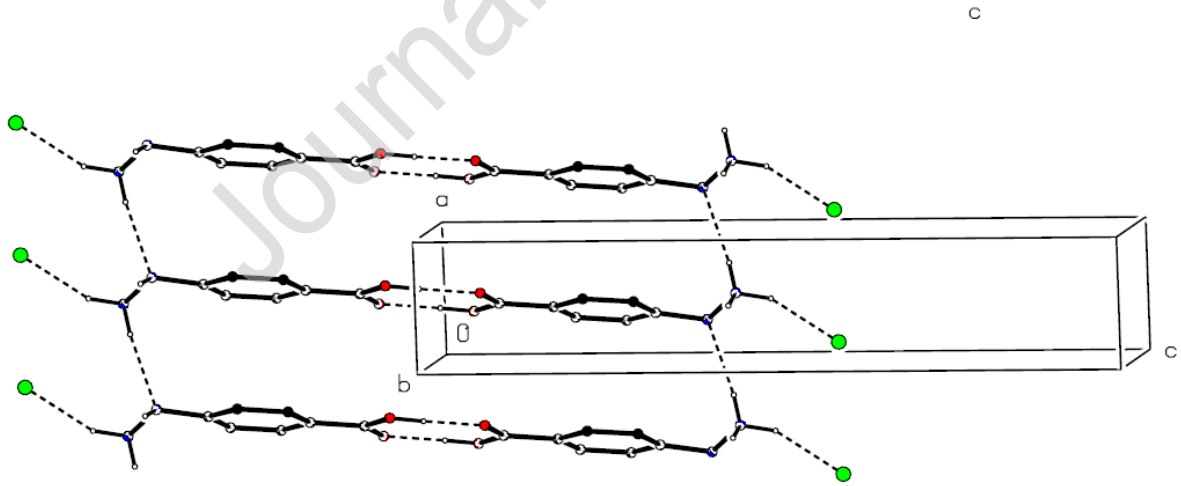

Figure 2. Part of the crystal structure of compound 4-HBA showing the formation of a hydrogen-bonded ladder running parallel to the [100] direction. Hydrogen bonds are shown

as dashed lines and, for the sake of clarity, the H atoms bonded to C atoms have been omitted.

The shorter component of the three-centre system involving atom H41 (Table 2) links the four-ion aggregates into a chain of rings running parallel to the [-101] direction in which $R^2_2(8)$ rings centred at (0.5 - n, 0.5, n) alternate with $R^2_4(8)$ rings centred at (n, 0.5, 0.5 - n), where n represents an integer in each case (Figure 3). Finally, the second component of the same three-centre N-H...Cl system links the four-ion aggregates into another chain of rings, this time running parallel to the [01-1] direction, with $R^2_2(8)$ rings centred at (0.5, 0.5 - n, n) alternating with $R^2_4(10)$ rings centred at (0.5, n, 0.5 - n), where n again represents an integer (Figure 4). The combination of chain motifs along [100] [0101] and [01-1] is sufficient to generate a continuous three-dimensional framework structure.

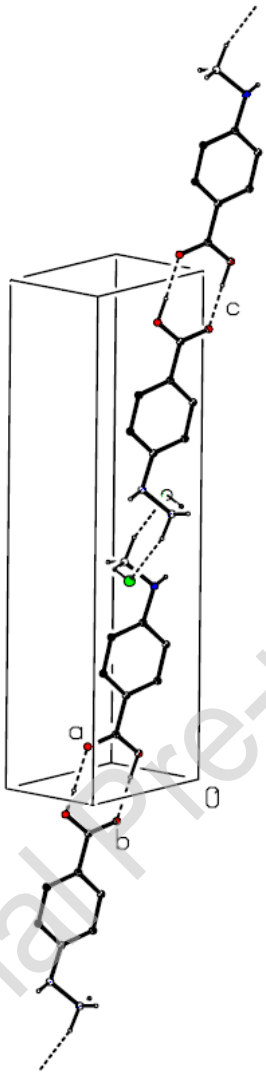

Figure 3. Part of the crystal structure of compound 4-HBA showing the formation of a hydrogen-bonded chain of rings running parallel to the [-101] direction. Hydrogen bonds are shown as dashed lines and, for the sake of clarity, the H atoms bonded to C atoms have been omitted.

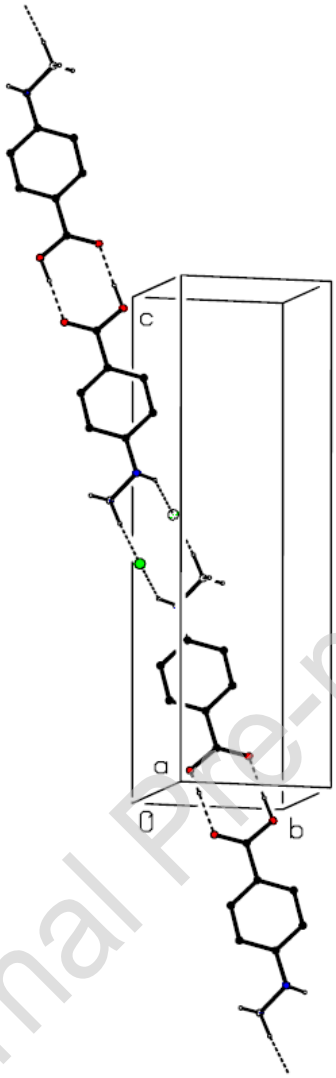

Figure 4. Part of the crystal structure of compound 4-HBA showing the formation of a hydrogen-bonded chain of rings running parallel to the [01-1] direction. Hydrogen bonds are shown as dashed lines and, for the sake of clarity, the H atoms bonded to C atoms have been omitted.

As indicated in Table 2, the chloride ion acts as an acceptor from five different cations and the coordination geometry at Cl (Figure 5) is best described as distorted square pyramidal. The Addison parameter τ_5, calculated from the H...Cl...H angles is 0.004: for ideal square pyramidal geometry, this parameter has the value zero, while for ideal trigonal bipyramidal geometry the value is unity.[38]

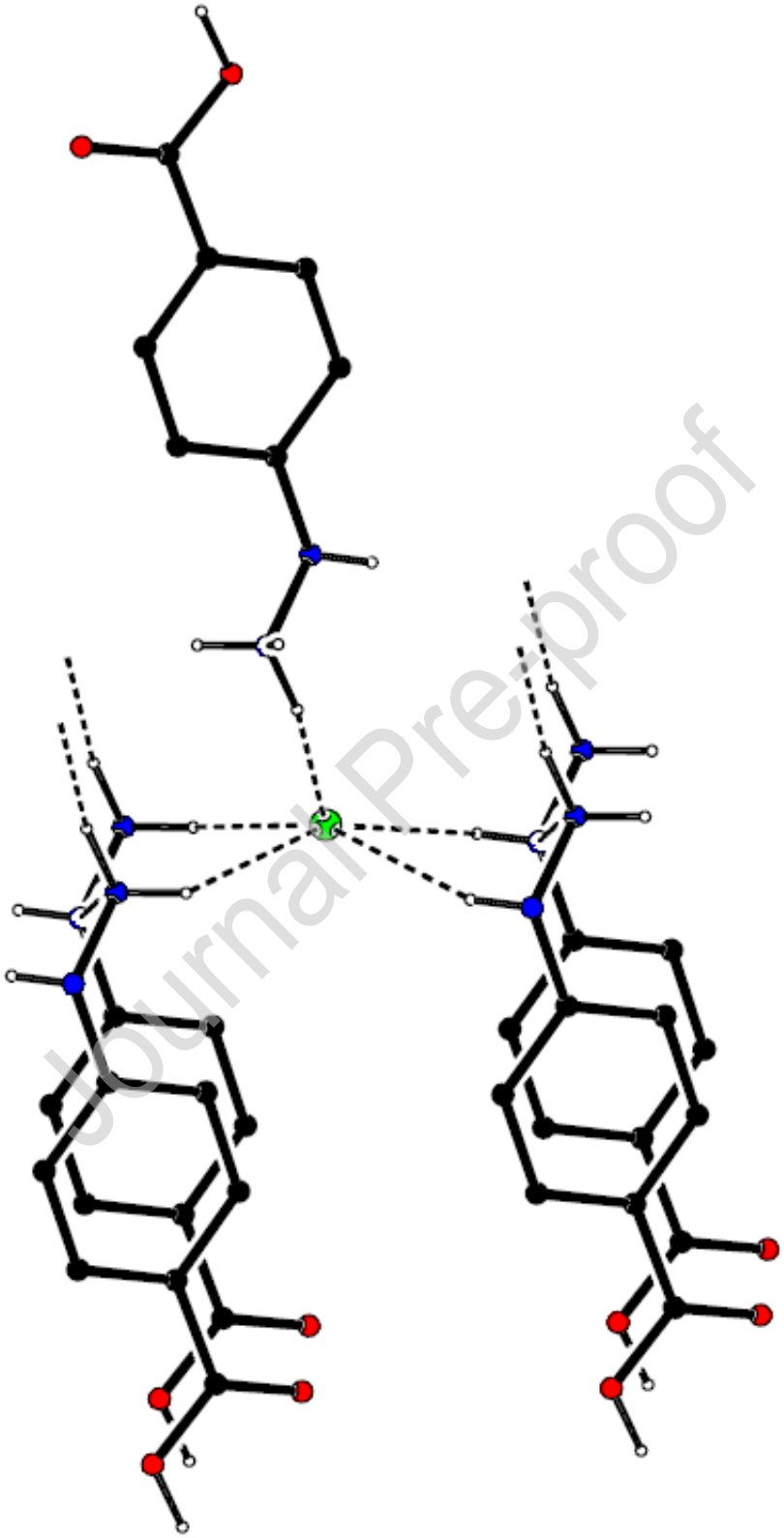

Figure 5. Part of the crystal structure of compound 4-HBA showing the coordination geometry around the chloride ion. For the sake of clarity, the H atoms bonded to C atoms have been omitted.

4.3. Molecular modeling of noncovalent interactions.

Based on the refined crystal structure, we constructed the molecular motif representing the unit cell, as can be observed in the Figure 6(a). Additionally, we modelled two molecular complexes with the most representative interactions. First, the symmetric hydrogen bonds between carboxylic acid moieties (see Figure 6(b)). Furthermore, a model with the π-stacking, NH···N and NH···Cl interactions can be observed in the Figure 6(c).

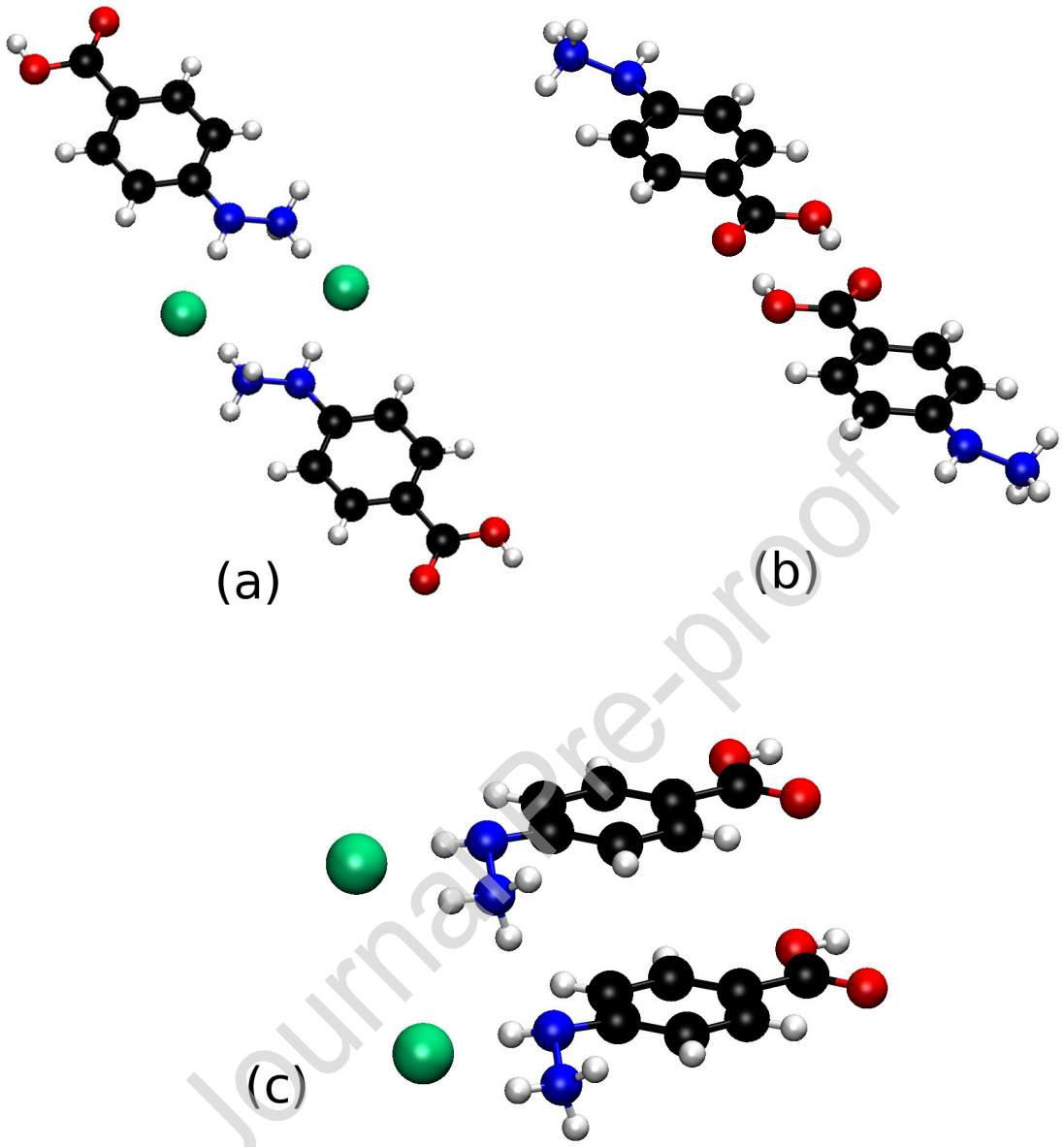

Figure 6. Representative models of (a) Unit cell; (b) Hydrogen bond interaction and (c) π-stacking of 4-HBA.

Figure 7 shows the NCIPlot of the unit cell. The value of sign(λ_2)ρ allows us identify three attractive interactions (color blue and magenta in Figure 7(a)). The isosurfaces in Figure 7(b) and (c) localized these interactions as the symmetric hydrogen bond between carboxylic groups (O1-H1···O2) and hydrogen bonding between N42-H42A···N41 and N42-H42B···Cl1. In Figure 8(b) y (c) these isosurfaces and sign(λ_2)ρ are shown in each

complex. A comparison with ethyl 4-hydrazinobenzoate hydrochloride (E-4HB) revealed similar interactions in the ammine and phenyl moieties [14].

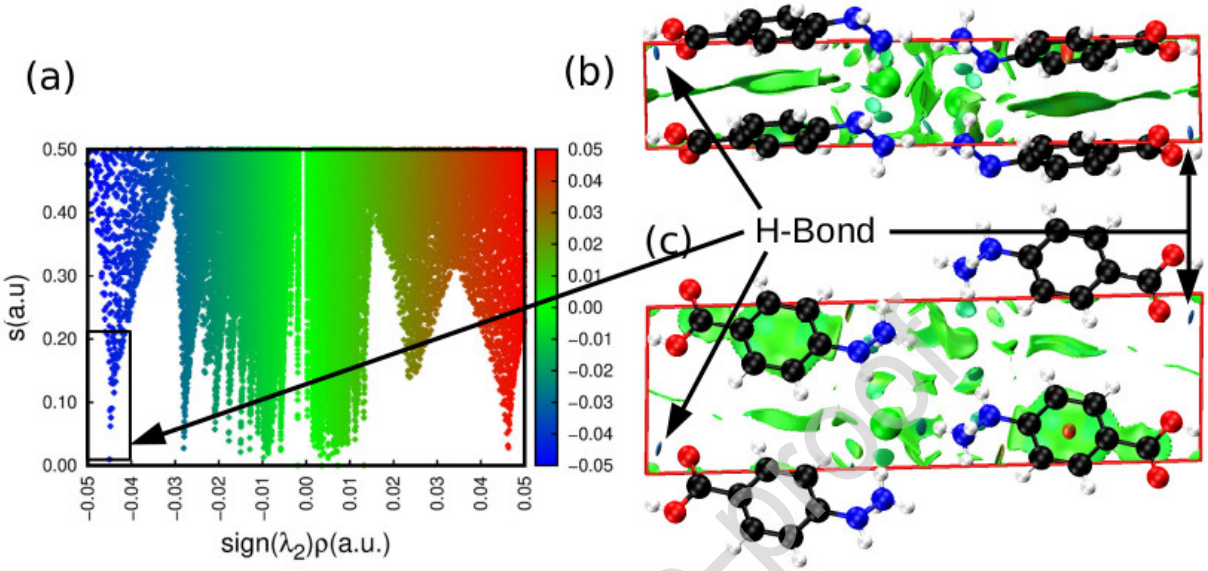

Figure 7. NCIplot of molecular motif of unit cell of 4-HBA.

The information of sign(λ_2)ρ, specifically NCI index, is related to the interaction energy as demonstrated by Contreras-García, Yang and Johnson for water clusters [39]. In this sense, we have observed the following in attractive interaction strength O1-H1···O2 (-0.045 au) > N42-H42A···N1 > N42-H42B···Cl1. Taking in account the repulsive contribution in the interaction region, we observed a low contribution given by pseudo-ring steric clash -- sign(λ_2)ρ ~ 0.008 au in Figure 8(b) -- O1-H1···O2. A similar behavior was reported for formic acid dimer [39]. In N42-H42A···N1 and N42-H42B···Cl1 interactions the repulsive contribution are given by the van der Waals interactions --- sign(λ_2)ρ between 0.00 and 0.01 au in Figure 8(c). Finally, the Coulombic repulsion between π-rings in the phenyl dimer leads to a parallel-displaced structure [35].

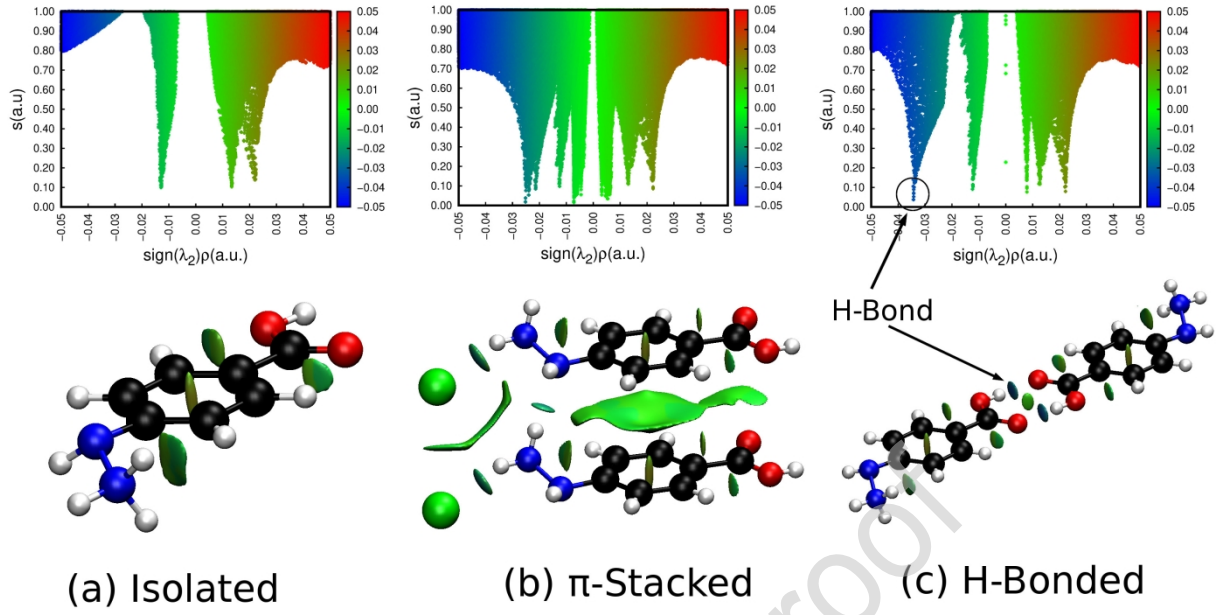

Figure 8. NCIPlots for representative models of interaction complexes of 4-HBA.

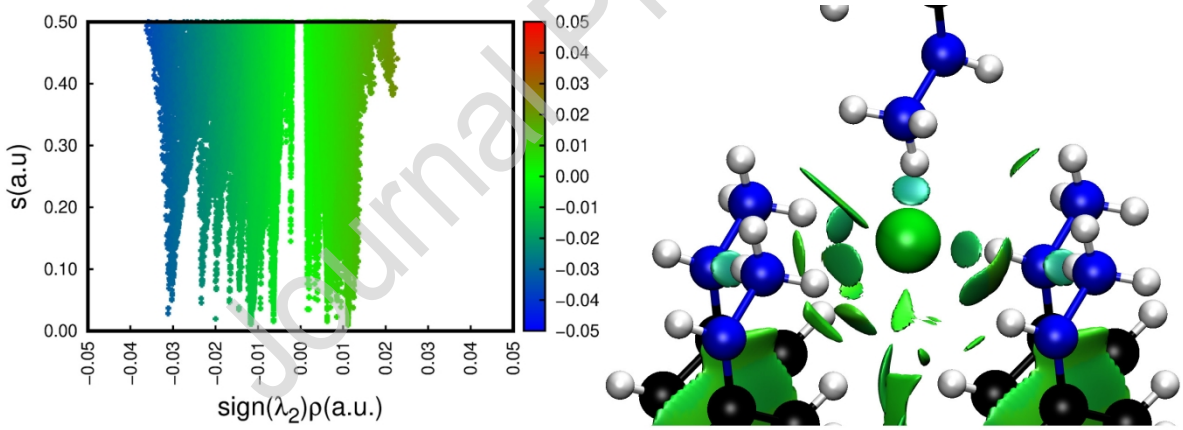

Figure 9. NCIPlot of geometrical region with specific interactions in 4-HBA.

The second most important interaction is around 0.031 au of sign(λ_2)ρ, it is shown in the bottom left of Figure 9. This region corresponds to the BH interactions N42-H42A···N41 and N42-H42B···Cl1. The first promotes the stacking of hydrazines shown in Figures 6(c). The latter represents the apex of the square-based pyramid previously discussed.

The rest of the attractive interactions involving hydrogen are between -0.025 and -0.015 au of sign(λ_2)ρ, and are consequence of the N42-H42C···Cl1 and the N41-H41···Cl1 interactions. Conversely to that observed in crystallography the N41-H41···Cl1 interaction has not significant attractive contribution, i.e. this NCI isosurface mainly contains repulsive interactions. This result explains the fact that N41–H41A···Cl1 and distance, from the NH fragment located at the top-left corner of the square-based pyramid of Figure 7 and central chloride, is large – 2.70 Å – see Table 2.

The last three interaction in the square-based pyramid are weakly interacting hydrogen bonds. The significant contribution of the repulsive interactions increases the bond length, e.g. the interaction between the N42 in the top-right corner of the base results in an H···Cl distance (2.70 Å) larger than the H···Cl in the N42 in the bottom-right corner (2.43 Å) – See Table 2. The volume of isosurface of the first region is smaller than the second region as can be compared in the bottom-left of Figure 9.

This balance between attractive and repulsive interaction tends to align the molecules toward the closest packing in the crystal.[40] Typically, the interactions between chloride and ammonium fragments has a stabilizing nature.[41] In this work, we have found a compensation between attractive and repulsive forces in the region of hydrogen bond domain, allowing chloride arrangements around ammonium and amine fragments. Finally, the stacked phenyl rings contains the repulsive and attractive van der Waals forces, i.e. values of sign(λ_2)ρ between -0.01 to 0.01 au. The isosurfaces revealed the delocalized nature of the π–π interactions.[42]

The results of searching critical points through the QTAIM analysis for the models of Figure 6 is shown in the Figure 10. In all cases, the Poincaré-Hopf condition in the number of critical points was fulfilled. The Table 3 shows the QTAIM properties of the (3,-1) critical points representing the important intermolecular noncovalent interactions in 4-HBA crystals. According to these results, all intermolecular interactions are characterized by low values of $\rho(r)$ and $\nabla^2\rho(r)$, typical for weak donor-acceptor interactions.[43] The non-covalency is confirmed by the $|V(r)|/G(r)$ values less than 1.

The values $\nabla^2\rho(r)$ and $|V(r)|/G(r)$ confirmed the behavior of relative strength of the interactions: O1-H1···O2 (HB01/02) > N42-H42A···N1 (PI06) > N42-H42B···Cl1 (PI07/03), observed with NCIPlot. Moreover, the ellipticity (ε) values close to zero indicate a nearly symmetrical distribution of charge density perpendicular to bond path, i.e. the π-character is low. The π-stacked model (Figure 10B) reveals the existence of weak interactions between the phenyl rings (PI01, PI02, PI04, PI05, PI08, PI10, PI11, PI13) with a high π character (ε > 0.2).

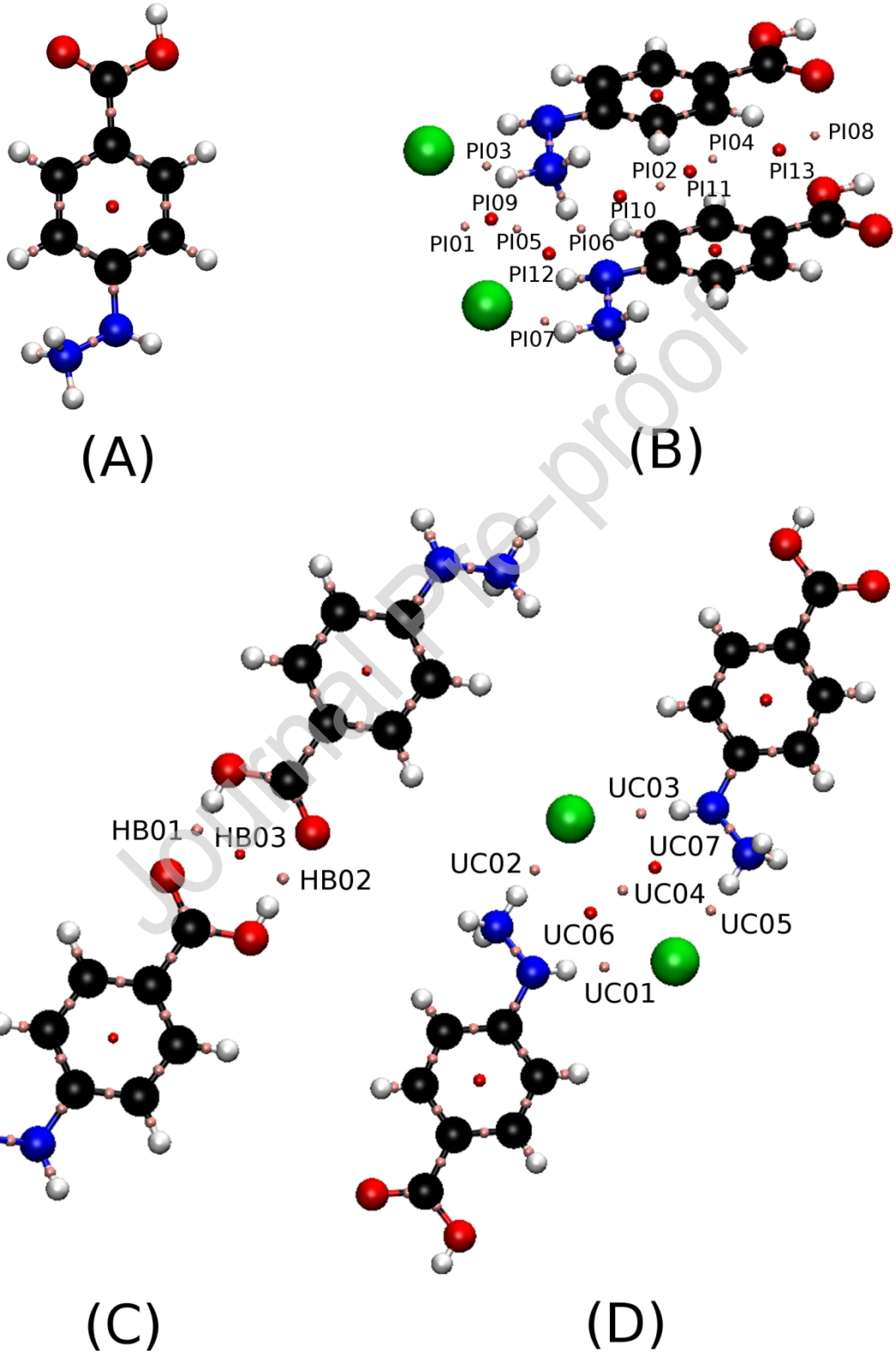

Figure 10. Critical points of the (A) isolated molecule; (B) π-stacking model; (C) Hydrogen bonded model; (D) unit cell. Pink and red spheres are (3,-1) and (3,+1) critical points, respectively. The critical points revealing the most significant noncovalents interactions are abbreviated as PI (π-stacking model), HB (Hydrogen bonded model) and UC (unit cell).

Table 3. QTAIM properties (au) of the (3,-1) critical points representatives of most important noncovalent intermolecular interactions of 4HBA.

Label	$\rho(r)\times10^3$	$\nabla^2\rho(r)\times10^2$	$\lvert V(r)\rvert/G(r)$	Ellipticity
HB01/02	34.34	15.35	0.8841	0.0115
PI01	6.489	1.585	0.8832	0.2335
PI02	7.197	1.835	0.8259	0.8681
PI03	24.01	6.192	0.9614	0.0218
PI04	6.723	1.766	0.8075	1.0345
PI05	6.048	1.830	0.8084	2.9566
PI06	21.58	6.948	0.9045	0.0265
PI07	25.23	6.092	0.9922	0.0212
PI08	4.536	1.738	0.8027	0.3316
UC01/03	13.21	3.900	0.9056	0.0668
UC02/05	23.02	6.373	0.9352	0.0248
UC04	3.828	0.8955	0.8490	0.6059

The decomposition of the total interaction energy of the models is presented in Table 4. In the H-bond and π-stacking models there is a high contribution of the steric repulsion energy. Since our models are based on the crystal structure, they implicitly contain the interactions of all the ionic components in the crystal. Consequently, the molecules are closer than should be, increasing the Pauli repulsion energy.

In the hydrogen-bond cyclic motifx, the electrostatic contribution (ΔE_{ES}) is small, contrary to expectation. In the literature, hydrogen-bonding interactions are generally characterized by a high contribution of the electrostatic term (ΔE_{ES}) because of charge transfer between donor and acceptor atoms.[44,45] However, Nemes, Laconsay and Galbraith point-out the

influence of Pauli repulsion between lone pairs on the donor and acceptor fragments for the destabilization of electrostatic interactions in the H-Bond.[46] Similar results were found for the model of π-stacking, while generally, the exchange interaction is the term with the highest contribution [47,48].

In the case of unit cell, the electrostatic contribution is high compared with the rest. The repulsion energy is compensated by exchange, polarization and dispersion energies. In summary, crystalline structure of 4-HBA is mainly stabilized by the electrostatic interactions between $NH_3^+\cdots Cl^-$ type, the hydrogen bond network around Cl^- and the strong N41-H41⋯N41 bond.

Table 4. Results of canonical molecular orbital energy decomposition analysis (CMO-EDA) for unit cell and, H-bonding and π-stacking complexes at the M06-2X/cc-pVDZ level (in kcal mol^{-1}).

	H-Bonded	π-stacking	Unit cell
ΔE_{es}	-0.80	3.16	-249.46
ΔE_{EX}	-14.30	-13.61	-30.06
ΔE_{REP}	45.71	45.94	83.86
ΔE_{POL}	-10.82	-8.33	-29.93
DFT ΔE_{DISP}	-10.78	-25.59	-24.00
E_{INT}	9.01	1.57	-249.59

5. Conclusions

The structural analysis of 4-HBA, was established by single crystal X-ray diffraction, and this is the first X-ray report of this compound. The component ions are linked two-centre hydrogen bonds of O-H..O, N-H...N and N-H...Cl types and by two different three-centre N-H...$(Cl)_2$ hydrogen bonds, such that the chloride ion accepts hydrogen bonds from five different cations in a square-pyramidal coordination geometry. The analysis of non-

covalent interactions showed that the coordination of the chloride ion is the consequence of the balance between H···Cl attractive and repulsive forces around the NH_3^+ and -NH- fragments, while the overall assembly depends not only upon the electrostatic interactions involving the chloride ions, but also upon an extensive series of π-interactions involving the aryl rings of the array of cations within the crystal, emphasizing the necessity of examining a wide variety of interaction types when assessing the non-covalent interactions as a whole.

6. Supplementary information

X-ray crystallographic data for this structure has been deposited at the Cambridge Crystallographic Data Center under code CCDC 1562625.

Acknowledgments

The authors thank Fondo Nacional de Ciencia, Tecnología e Innovación (FONACIT Proyecto de apoyo a Grupos No. G-2005000403). Proyecto 1063, Instituto Venezolano de Investigaciones Científicas (IVIC). N. Cubillan would like to thank Vicerrectoría de Investigaciones, Extensión y Proyección Social of Universidad del Atlántico (Grant CB20-FGI2016) for partial financial support of this work. We thank Dr. Duane Choquesillo-Lazarte (LEC, IACT-CSIC), for the data collection of compound 4-Hydrazinobenzoic acid hydrochloride (4-HBA).

References

[1] G.B. Kauffman, R.P. Ciula, Emil Fischer's discovery of phenylhydrazine, J. Chem. Educ. 54 (1977) 295. doi:10.1021/ed054p295.

[2] J. Berger, Phenylhydrazine haematotoxicity, J. Appl. Biomed. 5 (2007) 125–130.

[3] S. Harikrishna, K.N. Reddy, Y. Suresh, M. Ramakrishna, M. Sarat, K. Kishore, C. Rambabu, Low-level Determination of 4-Hydrazino Benzoic Acid in Drug Substance by High Performance Liquid Chromatography / Mass Spectrometry, E-Journal Chem. 7 (2010) 403–408. doi:http://dx.doi.org/10.1155/2010/616494.

[4] J. Wu, Q. Shi, Z. Chen, M. He, L. Jin, D. Hu, Synthesis and bioactivity of pyrazole acyl thiourea derivatives, Molecules. 17 (2012) 5139–5150. doi:10.3390/molecules17055139.

[5] A. Lévai, J. Jek, Synthesis of carboxylic acid derivatives of 2-pyrazolines, Arkivoc. (2007) 134–145. doi:http://dx.doi.org/10.3998/ark.5550190.0008.114.

[6] M. Morales-Toyo, Y.J. Alvarado, J. Restrepo, L. Seijas, R. Atencio, J. Bruno-Colmenarez, Synthesis, Crystal Structure Analysis, Small Cluster Geometries and Energy Study of (E)-Ethyl-4-(2-(thiofen-2-ylmethylene)hydrazinyl)benzoate, J. Chem. Crystallogr. 43 (2013) 544–549. doi:10.1007/s10870-013-0455-5.

[7] M. González, Y. Alvarado, J. Restrepo, J. Bruno-colmenárez, (E)-2-(4-methoxybenzylidene)-1-(2-nitrophenyl)hydrazine, Av. En Química. 8 (2013) 167–170.

[8] S. V Eliseeva, L.K. Minacheva, N.P. Kuz´mina, V.S. Sergienko, Crystal Structure of p -Carboxyphenylhydrazone Benzoylacetone, 50 (2005) 91–94.

[9] Y.J. Alvarado, A. Ballestas-Barrientos, N. Cubillán, M. Morales-Toyo, J. Restrepo, G. Ferrer-Amado, Preferential solvation of thiophene and furan-2-carboxaldehyde phenylhydrazone derivatives in DMSO-water and DMSO-n-octanol mixtures, Spectrochim. Acta - Part A Mol. Biomol. Spectrosc. 103 (2013) 361–367. doi:10.1016/j.saa.2012.10.057.

[10] P.A. Roussel, The Fischer indole synthesis, J. Chem. Educ. 30 (1953) 122. doi:10.1021/ed030p122.

[11] S. Gore, S. Baskaran, K. Burkhard, Fischer Indole Synthesis in Low Melting Mixtures, Org. Lett. 14 (2012) 4568–4571. doi:10.1021/ol302034r.

[12] ACD/ChemSketch, Freeware version 10.00, Adv. Chem. Dev. Inc., Toronto, ON, Canada. (2006). www.acdlabs.com.

[13] S. Rollas, Ş.G. Küçükgüzel, Biological activities of hydrazone derivatives, Molecules. 12 (2007) 1910–1939. doi:10.3390/12081910.

[14] J. Restrepo, C. Glidewell, N. Cubillán, Y. Alvarado, N. Dege, M. Morales-Toyo, Synthesis, crystal structure, and non-covalent interactions in ethyl 4-hydrazinobenzoate hydrochloride, J. Mol. Struct. 1177 (2019) 363–370. doi:10.1016/j.molstruc.2018.09.056.

[15] M. Morales-Toyo, C. Glidewell, J. Bruno-Colmenares, N. Cubillán, R. Sánchez-Colls, Y. Alvarado, J. Restrepo, Synthesis of (E)-Ethyl-4-(2-(furan-2-ylmethylene)hydrazinyl)benzoate, crystal structure, and studies of its interactions with human serum albumin by spectroscopic fluorescence and molecular docking methods, Spectrochim. Acta Part A Mol. Biomol. Spectrosc. 216 (2019) 375–384. doi:10.1016/j.saa.2019.03.028.

[16] N. Marom, R.A. Distasio, V. Atalla, S. Levchenko, A.M. Reilly, J.R. Chelikowsky, L. Leiserowitz, A. Tkatchenko, Many-body dispersion interactions in molecular crystal polymorphism, Angew. Chemie - Int. Ed. 52 (2013) 6629–6632. doi:10.1002/anie.201301938.

[17] P. Su, H. Li, Energy decomposition analysis of covalent bonds and intermolecular interactions, J. Chem. Phys. 131 (2009). doi:10.1063/1.3159673.

[18] E.R. Johnson, S. Keinan, P. Mori-Sánchez, J. Contreras-García, A.J. Cohen, W. Yang, Revealing noncovalent interactions, J. Am. Chem. Soc. 132 (2010) 6498–6506. doi:10.1021/ja100936w.

[19] J. Contreras-García, E.R. Johnson, S. Keinan, R. Chaudret, J.P. Piquemal, D.N. Beratan, W. Yang, NCIPLOT: A program for plotting noncovalent interaction regions, J. Chem. Theory Comput. 7 (2011) 625–632. doi:10.1021/ct100641a.

[20] J. Hernández-Paredes, R.C. Carrillo-Torres, A.A. López-Zavala, R.R. Sotelo-Mundo, O. Hernández-Negrete, J.Z. Ramírez, M.E. Alvarez-Ramos, Molecular structure,

hydrogen-bonding patterns and topological analysis (QTAIM and NCI) of 5-methoxy-2-nitroaniline and 5-methoxy-2-nitroaniline with 2-amino-5-nitropyridine (1:1) co-crystal, J. Mol. Struct. 1119 (2016) 505–516. doi:10.1016/j.molstruc.2016.05.012.

[21] G. Coleman, Phenylhydrazine, Org. Synth. 2 (1922) 71. doi:10.15227/orgsyn.002.0071.

[22] E.F.M. Stephenson, INDAZOLE, Org. Synth. 29 (1949) 54. doi:10.15227/orgsyn.029.0054.

[23] E. Stephenson, Indazole, Org. Synth. 29 (1949) 54. doi:10.15227/orgsyn.029.0054.

[24] Bruker, SADABS. Bruker AXS Inc., Madison, Wisconsin, USA. 2012., (2012).

[25] Bruker, APEX2. Bruker AXS Inc., Madison, Wisconsin, USA., (2013).

[26] G.M. Sheldrick, Crystal structure refinement with SHELXL, Acta Crystallogr. Sect. C Struct. Chem. 71 (2015) 3–8. doi:10.1107/S2053229614024218.

[27] G.M. Sheldrick, A short history of SHELX, Acta Crystallogr. Sect. A Found. Crystallogr. 64 (2008) 112–122. doi:10.1107/S0108767307043930.

[28] A.L. Spek, Structure validation in chemical crystallography, Acta Crystallogr. Sect. D Biol. Crystallogr. 65 (2009) 148–155. doi:10.1107/S090744490804362X.

[29] T. Lu, F. Chen, Multiwfn: A multifunctional wavefunction analyzer, J. Comput. Chem. 33 (2012) 580–592. doi:10.1002/jcc.22885.

[30] A. Otero-De-La-Roza, E.R. Johnson, V. Luaña, Critic2: A program for real-space analysis of quantum chemical interactions in solids, Comput. Phys. Commun. 185 (2014) 1007–1018. doi:10.1016/j.cpc.2013.10.026.

[31] N. Cubillan, https://github.com/njca12/ncirange (last accessed Dec 5 2017), NCIRange 1.0. (2017).

[32] W. Humphrey, A. Dalke, K. Schulten, {}: {Visual} molecular dynamics, J. Mol. Graph. 14 (1996) 33–38. doi:10.1016/0263-7855(96)00018-5.

[33] M.W. Schmidt, K.K. Baldridge, J.A. Boatz, S.T. Elbert, M.S. Gordon, J.H. Jensen, S. Koseki, N. Matsunaga, K.A. Nguyen, S. Su, T.L. Windus, M. Dupuis, J. John A. Montgomery, General Atomic and Molecular Electronic Structure System, J. Comput. Chem. 14 (1993) 1347–1363. doi:10.1002/jcc.540141112.

[34] A. Li, H.S. Muddana, M.K. Gilson, Quantum Mechanical Calculation of Noncovalent Interactions: A Large-Scale Evaluation of PMx, DFT, and SAPT Approaches, (2014).

[35] B. Brauer, M.K. Kesharwani, S. Kozuch, J.M.L. Martin, The S66x8 benchmark for noncovalent interactions revisited: explicitly correlated ab initio methods and density functional theory, Phys. Chem. Chem. Phys. 18 (2016) 20905–20925. doi:10.1039/C6CP00688D.

[36] P. Hobza, Calculations on noncovalent interactions and databases of benchmark interaction energies, Acc. Chem. Res. 45 (2012) 663–672. doi:10.1021/ar200255p.

[37] J. Bernstein, R.E. Davis, L. Shimoni, N. Chang, Patterns in Hydrogen Bonding: Functionality and Graph Set Analysis in Crystals, Angew. Chemie Int. Ed. English. 34 (1995) 1555–1573. doi:10.1002/anie.199515551.

[38] A.W. Addison, T.N. Rao, J. Reedijk, J. van Rijn, G.C. Verschoor, Synthesis, Structure, and Spectroscopic Properties of Copper(II) Compounds containing Nitrogen-Sulphur Donor Ligands ; the Crystal and Molecular Structure of Aqua[1,7-bis(N-methylbenzimidazol-2'-yl)- 2,6-dithiaheptane]copper(II) Perchlorate., J. Chem. SOC., Dalt. Trans. (1984) 1349–1356.

[39] J. Contreras-García, W. Yang, E.R. Johnson, Analysis of hydrogen-bond interaction potentials from the electron density: Integration of noncovalent interaction regions, J. Phys. Chem. A. 115 (2011) 12983–12990. doi:10.1021/jp204278k.

[40] A. Otero-de-la-Roza, E.R. Johnson, J. Contreras-García, Revealing non-covalent interactions in solids: NCI plots revisited, Phys. Chem. Chem. Phys. 14 (2012) 12165. doi:10.1039/c2cp41395g.

[41] A. Pajzderska, K. Drużbicki, A. Kiwilsza, M.A. Gonzalez, M. Jarek, J. Mielcarek, J. Wąsicki, On the relaxation dynamics in active pharmaceutical ingredients: solid-state 1 H NMR, quasi-elastic neutron scattering and periodic DFT study of acebutolol hydrochloride, RSC Adv. 5 (2015) 57502–57514. doi:10.1039/C5RA08937A.

[42] M. Alonso, T. Woller, F.J. Martín-Martínez, J. Contreras-García, P. Geerlings, F. De Proft, Understanding the fundamental role of dispersion interactions in shaping carbon-based materials, Chem. - A Eur. J. 20 (2014) 4931–4941. doi:10.1002/chem.201400107.

[43] M. Małecka, DFT studies and AIM analysis of intramolecular N-H···O hydrogen bonds in 3-aminomethylene-2 methoxy-5,6-dimethyl-2-oxo-2,3-dihydro-2λ5-[1,2]oxaphosphinin-4-one and its derivatives, Struct. Chem. 21 (2010) 175–184. doi:10.1007/s11224-009-9556-3.

[44] H. Zhao, S. Tang, S. Li, L. Ding, L. Du, Theoretical investigation of the hydrogen bond interactions of methanol and dimethylamine with hydrazone and its derivatives, Struct. Chem. 27 (2016) 1241–1253. doi:10.1007/s11224-016-0749-2.

[45] H. Zhao, Q. Zhang, L. Du, Hydrogen bonding in cyclic complexes of carboxylic acid–sulfuric acid and their atmospheric implications, RSC Adv. 6 (2016) 71733–71743. doi:10.1039/C6RA16782A.

[46] C.T. Nemes, C.J. Laconsay, J. Morrison Galbraith, Hydrogen Bonding from a Valence Bond Theory Perspective: The Role of Covalency, Phys. Chem. Chem. Phys. (2018). doi:10.1039/C8CP03920H.

[47] T. Sierański, The intricacies of the stacking interaction in a pyrrole–pyrrole system, Struct. Chem. 27 (2016) 1107–1120. doi:10.1007/s11224-015-0732-3.

[48] T. Sierański, Discovering the stacking landscape of a pyridine-pyridine system, J. Mol. Model. 23 (2017) 338. doi:10.1007/s00894-017-3496-4.

Highlights

In this article we can highlight the following:

- The synthesized compound is an intermediate for the synthesis of new compounds with pharmacological interest.

- There is little evidence in the literature on this type of derivatives and the first report is more than 50 years old.

- The crystallographic data reveal that compound 4-HBA form a complex three-dimensional framework structure between cations and anions.

- The crystallographic observations were confirmed through the results obtained with the non-covalent interactions calculations.

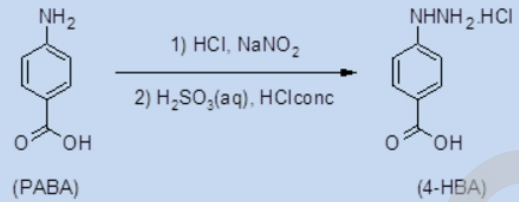
NH2
1) HCl, NaNO2
2) H2SO3(aq), HClconc
NHNH2.HCl
O
OH
(PABA)
(4-HBA)

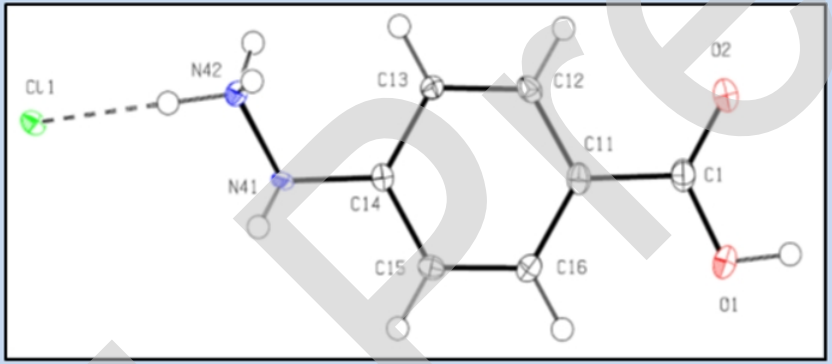
CL1
N42
N41
C13
C12
C14
C11
C1
O2
O1
C15
C16

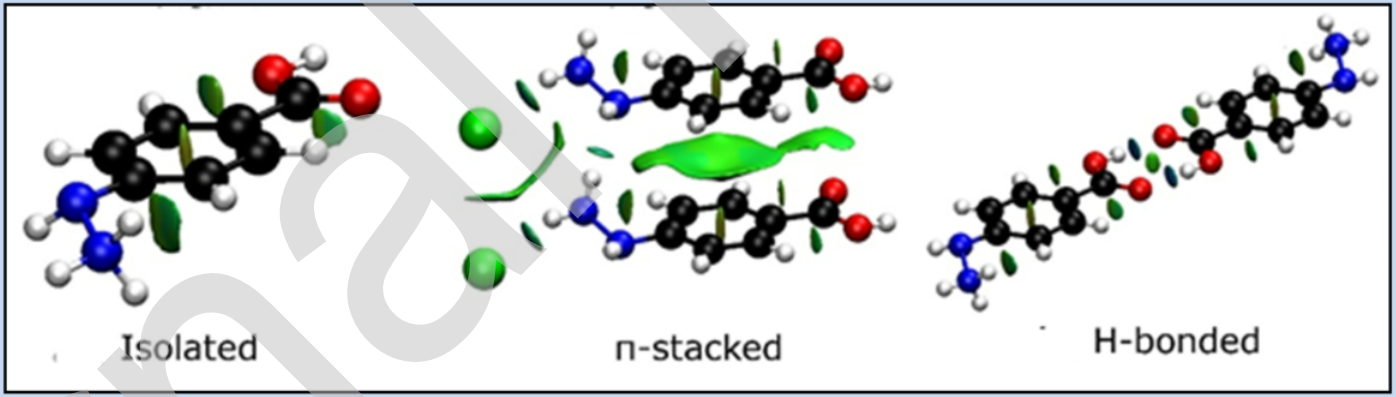
Isolated
π-stacked
H-bonded